Available online at www.sciencedirect.com
SCIENCE DIRECT®
Catalysis Today 89 (2004) 307–312
CATALYSIS TODAY
www.elsevier.com/locate/cattod

Optical and electrical properties of sputtered ZrN compounds

H.M. Benia [a], M. Guemmaz [a], G. Schmerber [b], A. Mosser [b], J.C. Parlebas [b,*]

[a] *DAC Laboratory, UFAS University, Sétif 19000, Algeria*
[b] *IPCMS, UMR7504, CNRS-ULP, 23 rue du Lœss, BP43, 67034 Strasbourg Cedex 2, France*

Abstract

We studied zirconium nitride layers prepared by reactive direct current (dc) magnetron sputtering and synthesized with nitrogen gas flow ranging from 1 to 9 sccm (standard centimeter cube per minute) N_2. We measured their electrical resistivity and recorded their X-ray diffraction patterns as well as their RBS spectra and optical reflectance curves. Thus we could determine their crystallographic structure, their nitrogen content and their optical properties by simulating the reflectance curves with Drude's model for stoichiometric and sub-stoichiometric samples, and an extended Drude model for over-stoichiometric samples. In this work, we focus on our stoichiometric sample S4, in order to compare the dielectric function as well as the optical indexes *n* and *k*, deduced from fit optical parameters, with those given in literature. There is a good agreement between these results. Besides, we determined the "optical resistivity" of our several samples and compared them with the "electrical resistivity" measured by a four-probe method. Also, a good agreement is found between both curves, which confirms that the formalism used to simulate the reflectance curves is well adapted to these compounds.

PACS: 2.60 ED; 72.15-v; 68.55-a; 78.20 Ci; 78.66 Bz

Keywords: Zirconium nitrides; Reflectance; Resistivity; Optical constants; Drude's model

1. Introduction

Thanks to their interesting properties (high melting point, chemical stability and corrosion resistance [1]), zirconium nitrides are used in different applied domains, notably as coatings [2–6], in cryogenic thermometers [7], in Josephson junctions [8], as gates in MESFET transistor technology [9], as diffusion barriers in p^+/n junctions [10] and in Cu/Si contacts [11,12] and finally as an attractive inert matrix in fast reactor fuels for incineration of plutonium and minor actinides [13].

In this paper, we investigate crystallographic, electrical and optical properties of various stoichiometric and non-stoichiometric zirconium nitrides prepared by dc reactive magnetron sputtering. Section 2 is devoted to the sample preparation and characterization, whereas in Section 3 we present and discuss our experimental results. In Section 4, we present the simulation method of the optical reflectance curves with use of Drude's model for sub-stoichiometric and stoichiometric samples, which was already used in several works [14,15], and an extended Drude model for over-stoichiometric samples [25]. The derived optical parameters are given in Table 2, and the dielectric function and the *n* and *k* indexes are compared with those found in literature in case of stoichiometric samples [4,14].

2. Samples preparation

The zirconium nitride samples were prepared by reactive magnetron sputtering. The target–substrates distance was 200 mm. A pure Zr disc (82.5 mm in diameter, 6 mm thick, 99.16% pure) was used as target. Polished single crystalline Si(1 0 0) surfaces were used as substrate and ultrasonically cleaned for 10 min successively in acetone and ethanol and finally dried in a N_2 gas jet. Prior to deposit, the system was pumped down to a pressure of about 6×10^{-8} Torr by a cryopump and the substrates as well as the target were sputter-cleaned for 30 min at 6×10^{-3} Torr and 20 min at 9×10^{-3} Torr, respectively. For Zr–N deposition, the plasma current was regulated at 800 mA in an argon gas flow of 20 sccm (4×10^{-3} Torr) and the nitrogen gas flow was varied from 0 to 9 sccm in order to obtain zirconium nitrides

* Corresponding author. Tel.: +33-3-88-10-70-74; fax: +33-3-88-10-72-49.
E-mail address: jean-claude.parlebas@ipcms.u-strasbg.fr (J.C. Parlebas).

0920-5861/$ – see front matter © 2004 Elsevier B.V. All rights reserved.
doi:10.1016/j.cattod.2003.12.006

Table 1
Deposition parameters and composition of ZrN_x films as measured by RBS

Sample	Nitrogen gas flow (sccm)	N/Zr atomic ratio
S0	0	0
S2	2	0.25
S4	4	1
S5	5	1.1
S7	7	1.2
S9	9	1.38

thin films with increasing nitrogen concentrations. Substrate temperature was fixed at 150 °C for all film depositions except for S0 which was deposited at 35 °C. The deposition parameters are reported in Table 1 (the samples are labeled as S[*i*], where *i* indicates the value of the nitrogen flow).

3. Experimental results

Rutherford backscattering spectrometry (RBS) [16] was used to determine the film composition and thickness of the layers. The experiments were carried out using a 2 MeV $^4H^{2+}$ ion beam. The backscattered spectra were analyzed using the simulation for analysis of materials (SAM) code. The crystal structure of the films was determined by X-ray diffraction (XRD). XRD spectra were recorded in the $\theta/2\theta$ mode, between $2\theta = 30^\circ$ and 80° with a step of 0.05° using monochromatic Cu $K\alpha_1$ radiation. Electrical resistivity was measured using a four-probe method. Optical reflectance spectra were recorded between 250 and 2500 nm with an UV-Vis-NIR photospectrometer. A commercial barium sulfate ($BaSO_4$) reference was used as blank reference for reflectance spectra measurements.

From XRD patterns we concluded that S0 and S2 samples crystallize in the α-Zr phase of hexagonal structure. For the other samples, the structure is cubic of NaCl type (δ-ZrN phase) and above the stoichiometry, which is obtained at 4 sccm nitrogen gas flow, the films become more and more amorphous, with a cell dilatation of the crystallized part due to the incorporation of nitrogen atoms in interstitial positions [17]. Fig. 1 shows the XRD pattern of the stoichiometric S4 film. We remark a good crystallization in the δ-ZrN phase with a cell parameter $a = 4.584$ Å.

The RBS spectra show that films with increasing nitrogen concentration from under- to over-stoichiometry (Table 1) [17] were synthesized and that the stoichiometry was reached nearly at 4 sccm N_2. It is well known that the ZrN stoichiometric compound, due to its special bonds, has a metallic behavior [8,18–20]. From Fig. 2 which shows the evolution of electrical resistivity of films as a function of nitrogen flow, one remarks that sample S4 presents a minimum of electrical resistivity (65.73 μΩ cm) in good agreement with its metallic behavior.

The increase of resistivity, when going from S0 to S2 samples, may be due to electron scattering by nitrogen molecules and atoms incorporated in the Zr lattice which play the role of impurities. The increase of resistivity beyond 4 sccm at high nitrogen gas flow suggests the formation of an insulating phase, probably amorphous Zr_3N_4 [21]. This is confirmed by the trend to amorphization which means a high presence of defects. Also, the increase of nitrogen concentration in the ZrN crystallites induces the stretching out of the cell and an increase of the electrical resistivity [17].

Besides, these zirconium nitride samples have various colors to the eye. Actually the color varies from metallic gray for low nitrogen flows to semi-transparent brownish for high nitrogen flows, with a golden yellow (sample S4), which is the normal color of stoichiometric ZrN compound. This last

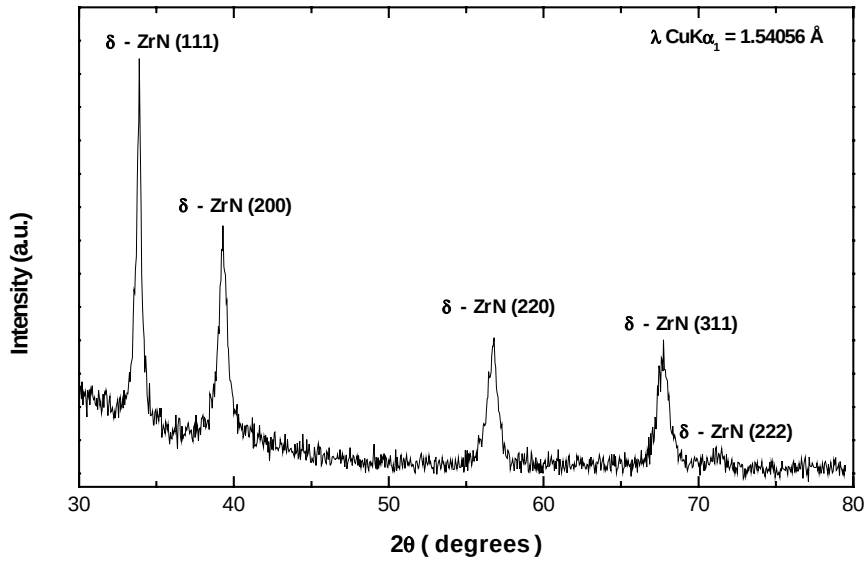

Fig. 1. X-ray diffraction pattern of the stoichiometric S4 sample.

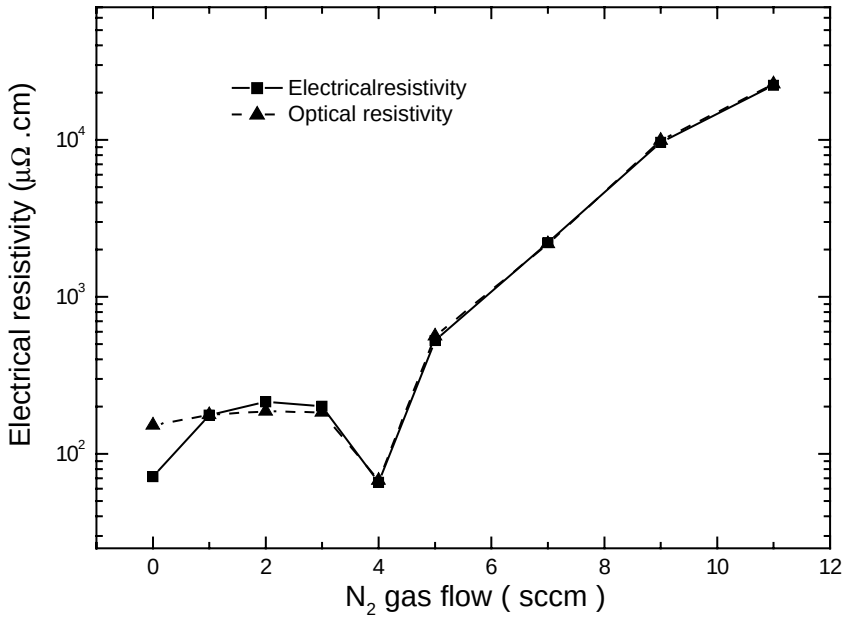

Fig. 2. Evolution of the electrical resistivities of ZrN_x films as a function of N_2 gas flow and correlation with the optical resistivities obtained after simulation of the reflectance spectra using the Drude or extended Drude models.

color is characterized by a minimum of reflectance (10%) in the visible domain (at ~365 nm) and a maximum (80%) in the infrared domain, which confirms promising use of these films in heat mirror industry [4].

4. Optical constants determination

The optical reflectance curves, corresponding to most samples, are given in Fig. 3. To determine their optical constants, we used the dielectric function given by Drude's model [22] for the sub-stoichiometric and stoichiometric samples (Eq. (1)) and by an extended Drude model for the over-stoichiometric samples in order to fit the reflectance spectra.

The dielectric function $\varepsilon_r(\omega)$ for a metal as a function of frequency ω is given by Drude's model:

$$\varepsilon_r(\omega) = \varepsilon_{hf}\left[1 - \frac{\omega_p'^2}{\omega^2 + i\omega/\tau}\right] \quad (1)$$

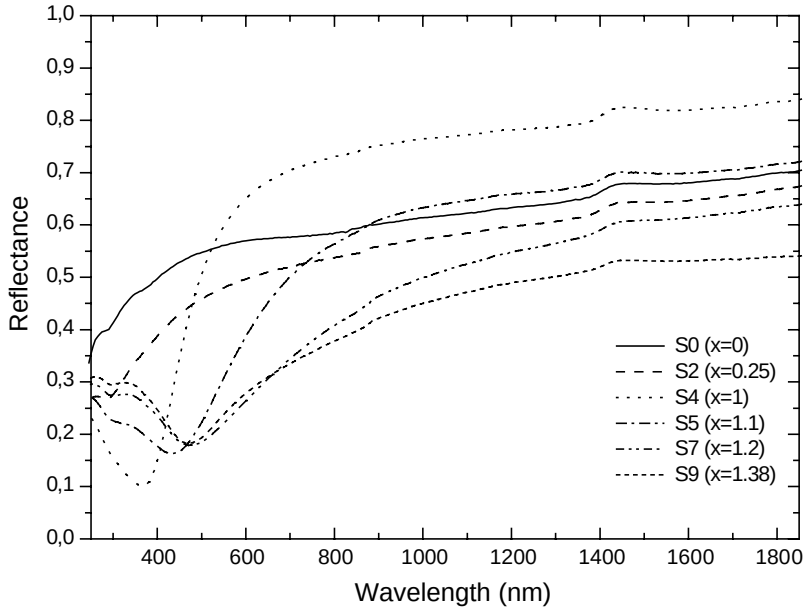

Fig. 3. Reflectance curves of different ZrN_x samples.

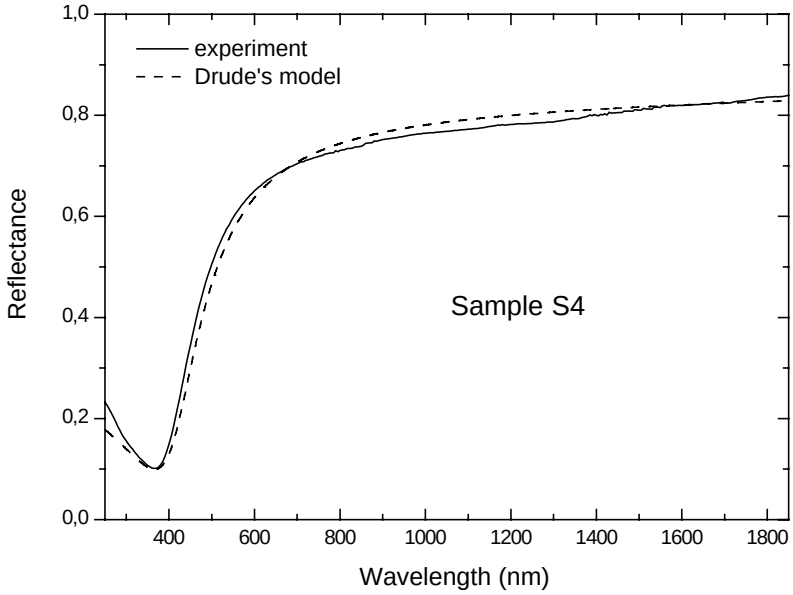

Fig. 4. Fit of the S4 sample reflectance spectrum using Drude's model.

where ε_{hf} is the high frequency dielectric constant, ω'_p the screened plasmon frequency and τ is the electron scattering time.

The reflectance R for normal incidence and a semi-infinite medium is provided by the Fresnel relation (2):

$$R = \left|\frac{1-\sqrt{\varepsilon_r}}{1+\sqrt{\varepsilon_r}}\right|^2 \quad (2)$$

In Fig. 4, we present the reflectance spectra of S4 sample with its fit curve deduced from Eqs. (1) and (2). We remark a good agreement between both curves. We deduce, from the fit that $\omega'_p = 4.62 \times 10^{15}$ Hz, $1/\tau = 5.61 \times 10^{15}$ Hz and $\varepsilon_{hf} = 11.2$. It is interesting to notice that the value of the screened plasmon frequency ω'_p is close to the value obtained, using also Drude's model, by Veszelei et al. [14] for a stoichiometric ZrN compound. The real and imaginary parts ε_1, ε_2 of the dielectric function for sample S4 have been derived from the optical fitted parameters (Fig. 5a) and compared to those derived by Karlsson et al. [4] using a Kramers–Kronig analysis (Fig. 5b). One observes a good agreement. The refraction index n and extinction coefficient k derived from the dielectric function through their usual definition $N = n + ik = (\varepsilon_r)^{1/2}$ are presented in Fig. 6. They are very similar to the results derived through ellipsometry in Ref. [14].

In the over-stoichiometric samples, the reflectance curves cannot be fitted with Drude's model alone, due to the fact that the resistance of these samples increases when the nitrogen concentration increases. For this reason, we assume that the dielectric function $\varepsilon_r(\omega)$ of over-stoichiometric samples is the sum of two parts. The first part, given by Drude's

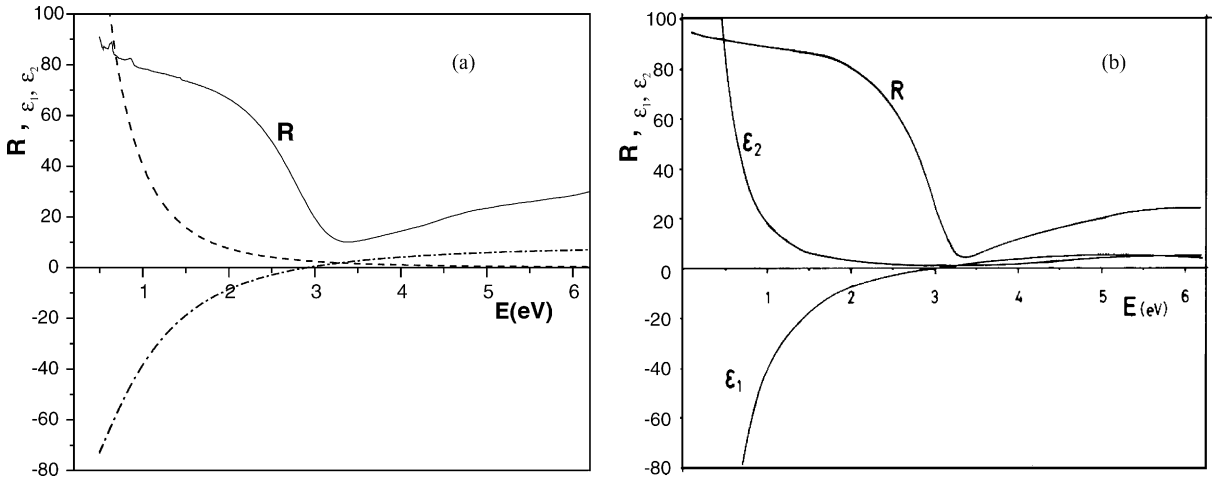

Fig. 5. Comparison between real and imaginary parts of the dielectric function for (a) sample S4 derived through Drude's analysis and (b) those for stoichiometric zirconium nitride CVD-coated films derived through a Kramers–Kronig analysis by Karlsson et al. [4].

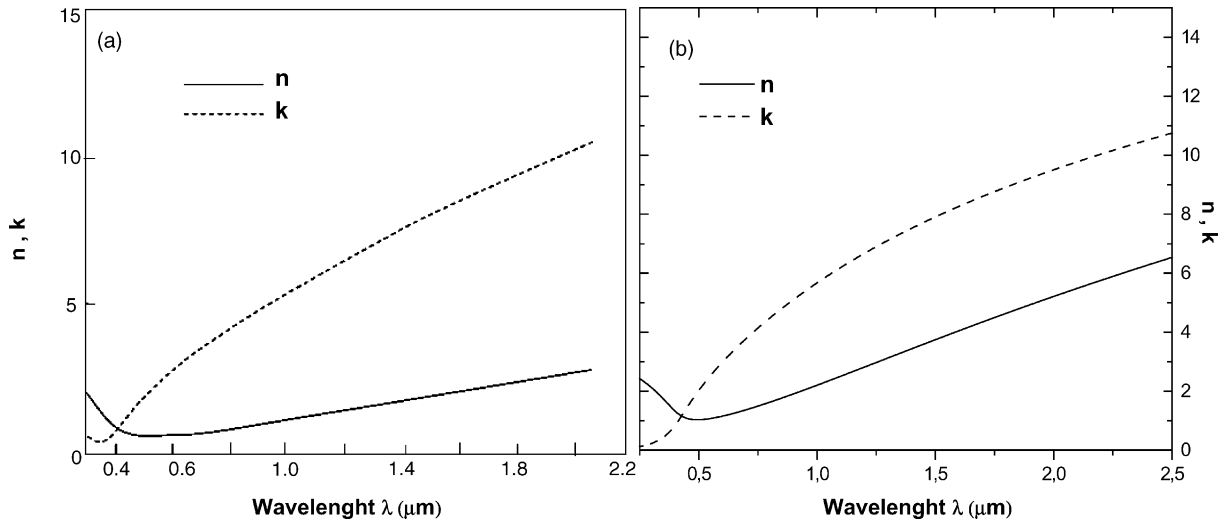

Fig. 6. Comparison of real n and imaginary k parts of the optical index $N = n + ik$ for the stoichiometric zirconium nitride sample: (a) using Drude's model according to Veszelei et al. [14] and (b) by fitting the reflectance curve for the stoichiometric S4 sample.

Table 2
Fitting parameters of the reflectance curves corresponding to the various ZrN_x films

Sample	ω'_p (10^{15} Hz)	$1/\tau$ (10^{15} Hz)	ε_m	ε_d	ω_t (10^{15} Hz)	Structure	Color
S0	9.0	6.0	10	0.0	0.0	Hexagonal	Gray
S1	8.4	11.4	10.3	0.0	0.0	Hexagonal	Gray
S2	5.7	6.6	12.3	0.0	0.0	Hexagonal	Gray
S3	5.55	5.61	11.2	0.0	0.0	NaCl	Gray
S4	4.62	1.3	10.2	0.0	0.0	NaCl	Yellow
S5	3.72	1.92	2.8	7.41	0.54	NaCl + amorphous	Yellow
S7	3.1	2.4	1.3	8.0	0.6	NaCl + amorphous	Yellow
S9	3.0	2.37	0.3	8.5	1.47	NaCl + amorphous	Brownish

model, represents the metallic behavior of the crystallized ZrN_x phase and the second part, given by a semiconductor model [23] represents the insulating behavior of the amorphous phase. This semiconductor model is characterized by an energy gap $E_g = \hbar\omega_t$ ($\hbar$ being Planck constant over 2π and ω_t a transition frequency) between valence and conduction band.

The dielectric function of the extended Drude model becomes

$$\varepsilon_r(\omega) = \varepsilon_m\left(1 - \frac{\omega_p'^2}{\omega^2 + i\omega/\tau}\right) + \varepsilon_d\left(1 - \frac{\omega_p'^2}{\omega^2 - \omega_t^2 + i\omega/\tau}\right) \quad (3)$$

Here, the plasmon frequency becomes $\omega_p^2 = \omega_p'^2(\varepsilon_m + \varepsilon_d)$.

The fit is clearly improved by using this extended model, and the fit parameters obtained in such a way appear in Table 2.

In Fig. 2, we correlate the optical resistivity determined for the various samples by using Eq. (4) for zero frequency ($\omega = 0$) (where the resistivity $\rho_1 = 1/\sigma_1$) [24] on one hand, and the electrical resistivity measured on the same samples by a four-probe method on the other hand:

$$\sigma_1 = \frac{\varepsilon_m}{4\pi}\tau\omega_p'^2 \quad (4)$$

The good agreement between both curves allows us to conclude that the formalism used to derive the optical constants is well adapted to these compounds. Besides, it confirms that the stoichiometric sample presents a minimum for the electrical resistivity compared to the other zirconium nitrides.

5. Conclusion

Sub-stoichiometric and over-stoichiometric zirconium nitride films were prepared by reactive dc magnetron sputtering by varying the nitrogen gas flow from 1 to 9 sccm during the deposition. Electrical resistivity and optical reflectance curves as well as XRD patterns and RBS measurements were performed on the different samples.

In order to determine the optical constants of our several layers, an extended Drude model was used to fit the reflectance spectrum. A good agreement was obtained between the dielectric function and the optical constants n and k determined for the stoichiometric sample (S4) and

previous data given in literature. Besides, the optical resistivity for the frequency $\omega = 0$, i.e. the static optical resistivity, was derived from the optical constants and compared to the electrical resistivity measured directly by a four-probe method. Also, a good agreement between electrical and optical resistivities could be achieved for all samples, which confirms that the formalism used to simulate the reflectance curves is well adapted to these compounds.

Acknowledgements

This work was supported by the French–Algerian CMEP Accord Programme No. 00-MDU-468.

References

[1] L.E. Toth, Transition Metal Carbides and Nitrides, Academic Press, New York, 1971.
[2] V.N. Zhitomirsky, R.L. Boxman, S. Goldsmith, I. Grimberg, B.Z. Weiss, N.A. Travitzky, Surf. Coat. Technol. 94/95 (1997) 207.
[3] W.C. Russell, J. Phys. II 5 (1995) C5–C127.
[4] B. Karlsson, R.P. Shimshok, B.O. Seraphin, J.C. Haygarth, Solar Energy Mater. 7 (1983) 401.
[5] W.D. Sproul, Thin Solid Films 107 (1983) 141.
[6] C. Mitterer, P.H. Mayerhofer, W. Waldhauser, E. Kelesoglu, P. Losbichler, Surf. Coat. Technol. 108/109 (1998) 230.
[7] T. Yotsuya, M. Yoshitake, T. Kodama, Cryogenics 37 (1997) 817.
[8] K. Schwarz, A.R. Williams, J.J. Cuomo, J.H.E. Harper, H.T.G. Hentzell, Phys. Rev. B 32 (1985) 8312.
[9] M. Wautelet, J.P. Dauchot, F. Debal, S. Edart, M. Hecq, J. Mater. Res. 11 (4) (1996) 825.
[10] Y. Igarashi, T. Yamaji, S. Nishikawa, Jpn. J. Appl. Phys. 29 (1990) L2337.
[11] B.M. Takeyama, T. Itoi, E. Aoyagi, A. Noya, Appl. Surf. Sci. 190 (2002) 450.
[12] B.M. Takeyama, A. Noya, K. Sakanishi, J. Vac. Sci. Technol. B 18 (2000) 1333.
[13] M. Burghartz, G. Ledergerber, H. Hein, R.R. Van der Laan, R.J.M. Konings, J. Nucl. Mater. 288 (2001) 233.
[14] M. Veszelei, K. Andresson, C.G. Ribbing, K. Järrendahl, H. Arwin, Appl. Opt. 33 (1994) 1993.
[15] K. Tanabe, H. Asano, Y. Kaoh, O. Michikami, J. Appl. Phys. 63 (1988) 1733.
[16] W.-K. Chu, J. W. Mayer, M.-A. Nicolet, Backscattering Spectroscopy, Academic Press, Orlando, 1978.
[17] H.M. Benia, M. Guemmaz, G. Schmerber, A. Mosser, J.-C. Parlebas, Appl. Surf. Sci. 200 (2002) 231.
[18] A. Dunand, H.D. Flack, K. Yvon, Phys. Rev. B 31 (1985) 2299.
[19] P. Blaha, J. Redinger, K. Schwarz, Phys. Rev. B 31 (1985) 2316.
[20] A. Neckel, Int. J. Quantum Chem. 23 (1983) 1317.
[21] B.O. Johansson, H.T.G. Hentzell, J.M.E. Harper, J.J. Cuomo, J. Mater. Res. 1 (1986) 442.
[22] P. Drude, Ann. Phys. 1 (1900) 566 (Leipzig);
P. Drude, Ann. Phys. 3 (1900) 369 (Leipzig).
[23] J. Casaux (Ed.), Physique du Solide, Masson, Paris, 1981, p. 273.
[24] H.M. Benia, M. Guemmaz, G. Schmerber, A. Mosser, J.-C. Parlebas, Appl. Surf. Sci. 201 (2003) 146.